JACS
JOURNAL OF THE AMERICAN CHEMICAL SOCIETY

Article

pubs.acs.org/JACS

A Family of Highly Efficient CuI-Based Lighting Phosphors Prepared by a Systematic, Bottom-up Synthetic Approach

Wei Liu,[†,∥] Yang Fang,[†,∥] George Z. Wei,[†] Simon J. Teat,[‡] Kecai Xiong,[†] Zhichao Hu,[†] William P. Lustig,[†] and Jing Li*[,†]

[†]Department of Chemistry and Chemical Biology, Rutgers University, 610 Taylor Road, Piscataway, New Jersey 08854, United States
[‡]Advanced Light Source, Lawrence Berkeley National Laboratory, Berkeley, California 94720, United States

Supporting Information

ABSTRACT: Copper(I) iodide (CuI)-based inorganic−organic hybrid materials in the general chemical formula of CuI(L) are well-known for their structural diversity and strong photoluminescence and are therefore considered promising candidates for a number of optical applications. In this work, we demonstrate a systematic, bottom-up precursor approach to developing a series of CuI(L) network structures built on CuI rhomboid dimers. These compounds combine strong luminescence due to the CuI inorganic modules and significantly enhanced thermal stability as a result of connecting individual building units into robust, extended networks. Examination of their optical properties reveals that these materials not only exhibit exceptionally high photoluminescence performance (with internal quantum yield up to 95%) but also that their emission energy and color are systematically tunable through modification of the organic component. Results from density functional theory calculations provide convincing correlations between these materials' crystal structures and chemical compositions and their optophysical properties. The advantages of cost-effective, solution-processable, easily scalable and fully controllable synthesis as well as high quantum efficiency with improved thermal stability, make this phosphor family a promising candidate for alternative, RE-free phosphors in general lighting and illumination. This solution-based precursor approach creates a new blueprint for the rational design and controlled synthesis of inorganic−organic hybrid materials.

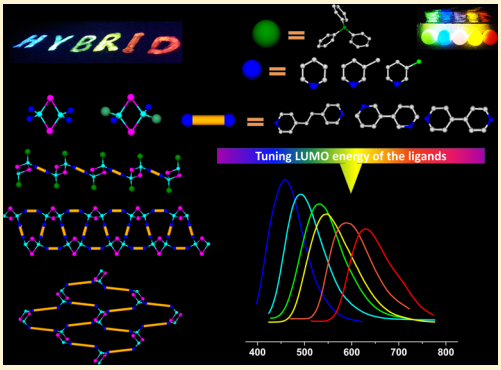

INTRODUCTION

The gradual replacement of traditional energy-costly incandescent light bulbs by compact fluorescent lamps (CFLs) and more recently by white light-emitting diodes (WLEDs) has been a crucial step toward reducing overall electrical consumption worldwide.[1] Incandescent lamps are extremely inefficient, as they convert only 3−5% of electric energy into light. A 60 W incandescent bulb is equivalent to a 14 W CFL or a 6 W WLED. In addition, the lifespans of CFLs and LEDs, up to 10,000 and 60,000 h, respectively, are significantly longer than that of an incandescent bulb, which is <3000 h.[2,3] Single or multicomponent phosphors are used in combination with either a glass tube filled with inert gas and a small amount of mercury (in the case of CFLs) or a blue, UV or near-UV LED chip (in the case of WLEDs) to generate white light of high quality.[4,5] A common example of this type of WLEDs, termed phosphor converted WLEDs or PC-WLED,[6,7] is made of a blue-emitting (455 nm) InGaN/GaN diode and a yellow-emitting (540 nm) YAG:Ce^{3+} phosphor, namely Ce^{3+}-doped yttrium aluminum garnet (YAG).[8] Similarly to YAG:Ce^{3+}, almost all commercial phosphors used in today's CFL and LED market are rare-earth (RE) metal-doped inorganic materials, including oxides, sulfides, oxysulfides, oxynitrides, and nitrides.[9,10] Advantages of these phosphors are high quantum efficiency and stability.[11] However, their dependence on RE elements, in particular europium, terbium, and yttrium, can become critical due to potential supply risk and cost issues.[12] In addition, their synthesis is often energy intensive, nonsolution processable, complex, and in need of high temperature (e.g., >1000 °C).[13,14] Because of these drawbacks, the development of new types of low-cost, energy-efficient, solution-processable, and RE-free phosphors is of immense importance.

Several groups of RE-free inorganic phosphors have been reported recently, such as ZnS, CdSe, nanocrystals, or quantum dots.[15−19] However, complicated synthetic procedure, relatively low quantum efficiency, and particle size dependence may limit their practical usages.[20−22] Hybrid materials built on inorganic semiconductor nanomodules and organic molecules combine the useful features of both components, giving rise to significant enhancement in their optical properties.[23−35] Among them, copper halide (I−VII) based hybrid materials are of particular interest due to their earth abundance (e.g., earth crust and seawater),[36] facile synthesis, structural diversity, and optical tunability and are thus considered promising phosphors for general lighting technologies.[37−40] However, there remain some

Received: May 15, 2015
Published: July 7, 2015

DOI: 10.1021/jacs.5b04840
J. Am. Chem. Soc. 2015, 137, 9400−9408

difficulties that must be resolved before their commercialization can be realized. For example, our previous investigations of one-dimensional (1D)-CuI(L) staircase-like chain structures showed that their internal quantum yields (IQY) are typically <40%, considerably lower than those of RE-based commercial phosphors (>70%).[7,39] Additionally, reactions often yield mixture phases containing different CuI modules. Therefore, developing a fully controllable synthesis to attain target structures with significantly improved IQYs has been the main focus of our most recent study.

In this work, we describe the design and rational synthesis of a family of copper iodide (CuI) hybrid structures built on Cu_2I_2 rhomboid dimer unit by a solution-based, bottom-up precursor approach. All compounds are constructed from highly emissive zero-dimensional (0D)-$Cu_2I_2(L)_4$ molecular precursors and have a general formula of $Cu_2I_2(L_1)_m(L_2)_n$ (L_1, L_2 = ligand). A range of structure types has been achieved, including 0D molecular clusters, 1D single- and double-chains, and two-dimensional (2D) layered networks. The precursor approach facilitates the formation of robust, extended network structures built on preselected inorganic modular units, while preventing the production of byproducts often unavoidable when using metal salt as reagent. The targeted hybrid structures have exceptionally high IQY (some >90%), well comparable to those of commercial phosphors. In addition, the band gaps and optical properties of the new $Cu_2I_2(L_1)_m(L_2)_n$ family can be systematically tuned, and their thermal and moisture stabilities are increased substantially from those of precursors, bringing them one step closer to the phosphor market.

EXPERIMENTAL SECTION

Materials. CuI (98%, Alfa Aesar), acetonitrile (>99%, Alfa Aesar), bulk acetone (>99%, Alfa Aesar), 3,5-dimethylpyridine (>98%, Alfa Aesar), 3-picoline (99%, Alfa Aesar), 3-cloro-pyridine (99%, Alfa Aesar), 1,2-bis(4-pyridyl)ethane (99%, Sigma-Aldrich), 1,3-bis(4-pyridyl)propane (98%, Alfa Aesar), 4,4′-dipyridyl sulfide (98%, TCI), 4,6-dimethyl-pyrimidine (>98%, TCI), (5-methyl-pyrimidine (98%, Alfa Aesar), 3,3′-bipyridine (98%, Alfa Aesar), 4,4′-bipyridine (98%, Alfa Aesar), triphenylphosphine (99%, Aldrich), pyrazine (98%, Alfa Aesar), 5-methyl-pyrimidine (98%, Alfa Aesar), 5-bromopyrimidine (98%, Alfa Aesar), sodium salicylate (99%, Merck), YAG:Ce^{3+} type 9800 (Global Tungsten & Powders Corp), and PolyOx N750 (Dow Chemical).

*Synthesis of 0D-Cu_2I_2(3-pc)$_4$ (3-pc = 3-Picoline) (**1**).* The synthesis of **1** was carried out by a modified version of the reported method.[41] CuI (0.19 g, 1.0 mmol) was first well-dispersed in 10 mL acetone in an open reaction vial, and 3-pc (0.37 g, 4.0 mmol) was slowly added under magnetic stirring at room temperature. Pure phase of the sample was collected by filtration after 10 min of continuous stirring. This compound was used as the precursor and was premade in large quantity for the synthesis of other structures. (Yield is 83% based on Cu.)

*Synthesis of 0D-Cu_2I_2(3,5-dm-py)$_4$ (3,5-dm-py = 3,5-Dimethyl-pyridine) (**2**).* Compound **2** was synthesized by a new precursor method developed in this work, which differs from the reported method.[42] 0D-Cu_2I_2(3-pc)$_4$ (**1**) was presynthesized as the precursor. **1** (0.15 g, 0.2 mmol) was first fully dissolved in 10 mL acetone in a glass vial to form a clear solution. Excess 3,5-dm-py (0.11 g, 1.0 mmol) in 2 mL acetone solution was slowly added under magnetic stirring at room temperature. The vial was then capped closely. Precipitate formed immediately and was collected after 10 min of stirring. (Yield is 70% based on Cu.) The same reaction set up was used for all other compounds unless otherwise mentioned.

*Synthesis of 0D-Cu_2I_2(3-Cl-py)$_4$ (3-Cl-py = 3-Chloro-pyridine) (**3**).* Single crystals of **3** were grown by leaving the mixed precursor/acetone with the 3-Cl-py solution in the open air undisturbed instead of stirring. Yellow rod-shaped crystals formed as acetone slowly evaporated. In a typical synthesis, **1** (0.15 g, 0.2 mmol) was fully dissolved in 10 mL acetone to form a clear solution. Then 3-Cl-py (0.50 g, 4.0 mmol) was slowly added. The reaction vial was sealed by plastic parafilm with some holes manually punched for the solvent to dry slowly. Pure phase of the sample formed when acetone was almost dried in 2 days. (Yield is 52% based on Cu.)

*Synthesis of 0D-Cu_2I_2(tpp)$_2$(3-pc)$_2$ (tpp = Triphenylphosphine) (**4**).* Compound **1** (0.15 g, 0.2 mmol) was dissolved in 10 mL acetone and mixed with tpp (0.13 g, 0.5 mmol) in 2 mL toluene. The solution remained clear after the mixing. Cubic crystals formed in several minutes at the bottom. High-quality crystals suitable for single-crystal X-ray diffraction (SCXRD) were collected after 6 h. Pure powder samples were obtained by directly mixing **1** (0.15 g, 0.2 mmol)/acetone (10 mL) solution with excess amount of tpp (0.13 g, 0.5 mmol) in 2 mL toluene under magnetic stirring. Precipitate formed within several minutes and was kept under stirring for 2 h before collected by filtration. This compound was used as the precursor for the preparation of powder samples of tpp-based structures. (Yield is 79% based on Cu.)

*Synthesis of 0D-Cu_2I_2(tpp)$_2$(4,6-dm-pm)$_2$ (4,6-dm-pm = 4,6-Dimethyl-pyrimidine) (**5**).* Compound **1** (0.15 g, 0.2 mmol) was first dissolved into 10 mL acetone, and then tpp (0.13 g, 0.5 mmol) and 4,6-dm-pm (0.06 g, 0.5 mmol) in 5 mL toluene solution was then added slowly. Crystals suitable for SCXRD were formed after 1 day. Pure phased powder samples were synthesized by directly mixing **4** (0.11 g, 0.1 mmol)/toluene with excess 4,6-dm-pm (0.06 g, 0.5 mmol) in toluene under magnetic stirring. Pure phase of sample was collected after 6 h. (Yield is 57% based on Cu.)

*Synthesis of 1D-Cu_2I_2(tpp)$_2$(bpp) (bpp = 1,3-bis(4-Pyridyl)-propane) (**6**).* Single crystals of **6** were obtained by the precursor method described above. Compound **1** (0.15 g, 0.2 mmol) was used as the precursor and was first dispersed in 10 mL acetone. Excess tpp (0.13 g, 0.5 mmol) and bpp (0.10 g, 0.5 mmol) were then added to the solution, and cubic crystals formed in 2 days at 80 °C. Pure powder samples were obtained by mixing **4** (0.11 g, 0.1 mmol) with excess bpp (0.10 g, 0.5 mmol) in 10 mL toluene under stirring at 80 °C. The targeted product was collected after 6 h. (Yield is 75% based on Cu.)

*Synthesis of 1D-Cu_2I_2(tpp)$_2$(4,4′-dps) (4,4′-dps = 4,4′-Dipyridyl sulfide) (**7**).* Compound **1** (0.15 g, 0.2 mmol) was used as the precursor and dissolved in 10 mL acetone. Then tpp (0.13 g, 0.5 mmol) and 4,4′-dps (0.09 g, 0.5 mmol) in 2 mL toluene was added to the above solution. The reaction solution remained clear after the mixing, and rod-shaped crystals formed in 1 h. Pure powder sample was obtained by directly mixing **4** (0.11 g, 0.1 mmol) with 4,4′-dps (0.09 g, 0.5 mmol) in toluene under magnetic stirring at room temperature. The product formed in 10 min and was collected after 3 h of stirring. (Yield is 81% based on Cu.)

*Synthesis of 1D-Cu_2I_2(tpp)$_2$(4,4′-bpy) (4,4′-bpy = 4,4′-Bipyridine) (**8**).* Precursor method, which is different from the reported method, was used to synthesize this compound.[43] Pure powder sample was obtained by mixing **4** (0.11 g, 0.1 mmol) with excess 4,4′-bpy (0.08 g, 0.5 mmol) in 10 mL toluene followed by heating at 80 °C for 12 h. (Yield is 75% based on Cu.)

*Synthesis of 1D-Cu_2I_2(tpp)$_2$(5-Br-pm)$_2$ (5-Br-pm = 5-Bromo-pyrimidine) (**9**).* Compound **1** (0.15 g, 0.2 mmol) was first dissolved in 10 mL acetone, and then mixed with tpp (0.13 g, 0.5 mmol) and 5-Br-pm (0.08 g, 0.5 mmol) in 10 mL toluene. The reaction was kept at 80 °C for 1 day. (Yield is 52% based on Cu.)

*Synthesis of 1D-Cu_2I_2(tpp)$_2$(pz) (pz = Pyrazine) (**10**).* Phase-pure powder sample was obtained by precursor method similar to the above and different from the reported procedure.[44] Compound **4** (0.11 g, 0.1 mmol) was mixed with excess pz (0.04 g, 0.5 mmol) in 10 mL toluene and kept at 80 °C for 1 day. (Yield is 67% based on Cu.)

*Synthesis of 1D-Cu_2I_2(5-me-pm)$_2$ (5-me-pm = 5-Methyl-pyrimidine) (**11**).* Single crystals were prepared by slow diffusion of 5-me-pm (0.05 g, 0.5 mmol) with **1** (0.15 g, 0.2 mmol) in 10 mL acetone solution. Rod-shaped crystals formed in 2 days. Pure powder sample was obtained by directly mixing 5-me-pm (0.09 g, 1.0 mmol) with **1** (0.76 g, 1.0 mmol)/acetone under magnetic stirring. The reaction was

DOI: 10.1021/jacs.5b04840
J. Am. Chem. Soc. 2015, 137, 9400−9408

kept overnight and was collected by filtration. (Yield is 64% based on Cu.)

*Synthesis of 1D-Cu_2I_2(5-Br-pm)$_2$ (**12**).* Slow diffusion of an 5-Br-pm (0.08 g, 0.5 mmol) and **1** (0.15 g, 0.2 mmol) in 10 mL acetone solution at room temperature led to the formation of pure-phased sample containing rod-shaped crystals in 3 days. (Yield is 58% based on Cu.)

*Synthesis of 2D-Cu_2I_2(bpe)$_2$ (bpe = 1,2-bis(4-Pyridyl)ethane) (**13**).* Different from the reported method, the precursor approach was applied.[45] **1** (0.15 g, 0.2 mmol) was fully dissolved in 10 mL acetone and slowly added to bpe (0.38 g, 2.0 mmol) in 2 mL acetone solution at room temperature under stirring in a closely capped reaction vial. Excess amount of ligand was used to ensure complete ligand exchange. Precipitate formed quickly and was collected by filtration after 30 min of continuous stirring. (Yield is 60% based on Cu.)

*Synthesis of 2D-Cu_2I_2(3,3′-bpy)$_2$ (3,3′-bpy = 3,3′-Bipyridine) (**14**).* Single crystals of **14** were grown by slow diffusion of 3,3′-bpy (0.16 g, 1.0 mmol) in 2 mL CH_2Cl_2 into **1** (0.15 g, 0.2 mmol) in 10 mL acetone solution. Green plate-like crystals suitable for SCXRD analysis formed in 3 days. Pure powder sample was obtained by directly mixing 3,3′-bpy (0.16 g, 1.0 mmol) with **1** (0.76 g, 1.0 mmol)/acetone solution. (Yield is 65% based on Cu.)

*Synthesis of 2D-Cu_2I_2(4,4′-dps)$_2$ (4,4′-dps = 4,4′-Dipyridyl sulfide) (**15**).* In contrast to the previous method, single crystals of **16** were prepared by mixing **1** (0.38 g, 0.5 mmol)/acetone with excess 4,4′-dps (0.19 g, 1.0 mmol)/acetone and leaving the reaction mixture undisturbed.[46] Rod-shaped crystals formed in 2 days. Pure powder sample was prepared by mixing 4,4′-dps (0.38 g, 2.0 mmol)with **1** (0.38 g, 0.5 mmol) in 20 mL acetone under magnetic stirring. (Yield is 68% based on Cu.)

*Synthesis of 2D-Cu_2I_2(4,4′-bpy)$_2$ (**16**).* Precursor method was used for synthesis this compound, which is different from reported method.[47] Pure powder sample was prepared by slowly mixing **1** (0.15 g, 0.2 mmol) in 10 mL acetone with 4,4′-bpy (0.08 g, 0.5 mmol) in 10 mL acetone under magnetic stirring at room temperature for 30 min. (Yield is 88% based on Cu.)

*Preparation of Blue and Yellow Phosphor Blend (**17**).* White light-emitting samples can be achieved by blending a blue emitting phosphor (**6**) with a yellow emitting phosphor (**8**). In a typical case, different weight ratio of compounds **6** and **8** were mixed mechanically in solid state. An optimum mixture phase was achieved at 75 wt % of **6** and 25 wt % of **8**, which was labeled as compound **17**.

Scale-up Synthesis. Larger amount of powder sample of compound **1** can be obtained by directly mixing bulk CuI with an excess amount of the ligand. CuI (19 g, 0.1 mol) was well dispersed in 100 mL acetone and excess 3-pc (37 g, 0.4 mol) was added. The reaction mixture was kept under magnetic stirring at room temperature for 30 min and then let acetone slowly dry out. Final product was collected after filtration, washing, and drying. (Yield is 76% based on Cu.) Other compounds can also be prepared in large scale using **1** as precursor. Take compound **4** as an example. Tpp (1.31 g, 5 mmol) in acetone was added to **1** (1.52 g, 2 mmol) in 100 mL acetone solution under magnetic stirring. Precipitate formed in several minutes, and the product was collected after 2 h of continuous stirring. (Yield is 71% based on Cu.)

Sample Washing and Drying. Upon completion of reactions, powder samples were collected by filtration from the reaction solution and washed with a small amount of acetone three times. These samples were then dried in a vacuum oven overnight before other measurements were made.

Single Crystal X-ray Diffraction (SCXRD). Single crystal X-ray diffraction data of **4**, **11**, **12**, and **14** were collected at low temperature (100 K) on a Bruker-AXS smart APEX CCD diffractometer with graphite-monochromated Mo Kα radiation (λ = 0.71073 Å). Single crystal data of **3**, **5**, **6**, 7, and **9** were collected at 150 K for **3**, **5**, and **9**; 298 K for **6**; and 230 K for **7** on a D8 goniostat equipped with a Bruker PHOTON100 CMOS detector at the Advanced Light Source (ALS), Lawrence Berkeley National Laboratory, using synchrotron radiation (λ = 0.7749 Å for **3**, **5**, and **6**; λ = 0.7085 Å for **7** and λ = 0.7293 Å for **9**). The structures were solved by direct methods and refined by full-matrix least-squares on F2 using the Bruker SHELXTL package. These data can be obtained free of charge from The Cambridge Crystallographic Data Centre via https://summary.ccdc.cam.ac.uk/structure-summary-form. The structures were deposited in Cambridge Structural Database (CSD) with numbers: 1062130−1062137 and 1062286. A brief summary of crystal data of all nine compounds are listed in Tables S1 and S2.

Powder X-ray Diffraction (PXRD). PXRD patterns of all compounds were collected on a Rigaku Ultima-IV automated diffraction system with Cu Kα radiation (λ = 1.5406 Å). Measurements were made in a 2θ range of 3−50° at room temperature with a step of 0.02° (2θ) and a counting time of 0.2 s/step. The operating power was 40 kV/44 mA.

Optical Diffuse Reflectance Measurements. Optical diffuse reflectance spectra were obtained on a Shimadzu UV-3600 spectrophotometer at room temperature. Data were collected in the wavelength range of 300−1000 nm. $BaSO_4$ powder was used as a standard (100% reflectance). The same analysis procedure was used to collect and convert the data using the Kubelka−Munk function. The scattering coefficient (S) was treated as a constant as the average particle size of the samples used in the measurements was significantly larger than 5 μm.

Thermogravimetric (TG) Analysis. TG analyses of the compounds were performed on a computer-controlled TG Q5000IR analyzer (TA Instrument). Pure powder samples were loaded into platinum pans and heated with a ramp rate of 10 °C/min from room temperature to 400 °C under nitrogen flow.

Photoluminescence (PL) Emission Measurements. Photoluminescence experiments were performed on a Varian Cary Eclipse spectrophotometer at room temperature. Samples were uniformly coated onto glass slides which do not emit in the visible light region.

Internal Quantum Yield (IQY)Measurements. The IQY of samples in powder form was measured on a C9920−03 absolute quantum yield measurement system (Hamamatsu Photonics) with a 150 W xenon monochromatic light source and 3.3 in. integrating sphere. Sodium salicylate and YAG:Ce^{3+} were chosen as the standards with an IQY of 60% and 95% at 360 and 455 nm, respectively.[48,49] Their IQY values were measured to be 64% and 97%, respectively.

Luminescence Decay Measurements. Luminescence lifetime was measured at room temperature by a FLS920 Edinburgh fluorimeter (Edinburgh Instruments, Livingston, United Kingdom) with a microsecond μF900 xenon flash lamp as the excitation resource and by time-correlated single photon counting. Instrumental response function (IRF) was applied to eliminate the influence from excitation source.

DFT Calculations. Band structure (BS) and density of states (DOS) calculations were performed on selected 0D, 1D, and 2D structures employing density functional theory (DFT). The electronic properties of ligands were evaluated with the DFT computation using Gaussian 09 at B3LYP/6-311++G(3df,3pd).[50−52]

Phosphor Coating and Fabrication of LED Bulbs. A water solution of binder (PolyOx N-750, 0.2 wt %) was made and stirred at room temperature for 6 h. In a typical preparation, selected phosphor (5.0 g) was added into 10 mL solution and well dispersed by stirring. The solution mixture was then applied onto the internal surface of a glass bulb and allowed to dry in open air. Mild heating was helpful to accelerate the drying process. This process was then repeated three times to ensure uniform coating.

RESULTS AND DISCUSSION

Designing Strategy and Bottom-Up Synthetic Approach. Our previous work shows reactions of CuI with pyridine-based ligands may lead to a number of different products, including 0D-$Cu_2I_2(L)_4$ dimers, 0D-$Cu_4I_4(L)_4$ tetramers, and 1D-CuI(L) staircase-like chain structures. Among them, 0D-$Cu_2I_2(L)_4$ dimers generally have the highest emission intensity and IQY, while higher-dimension compounds (e.g., 1D and 2D structures) are more stable. However,

DOI: 10.1021/jacs.5b04840
J. Am. Chem. Soc. 2015, 137, 9400−9408

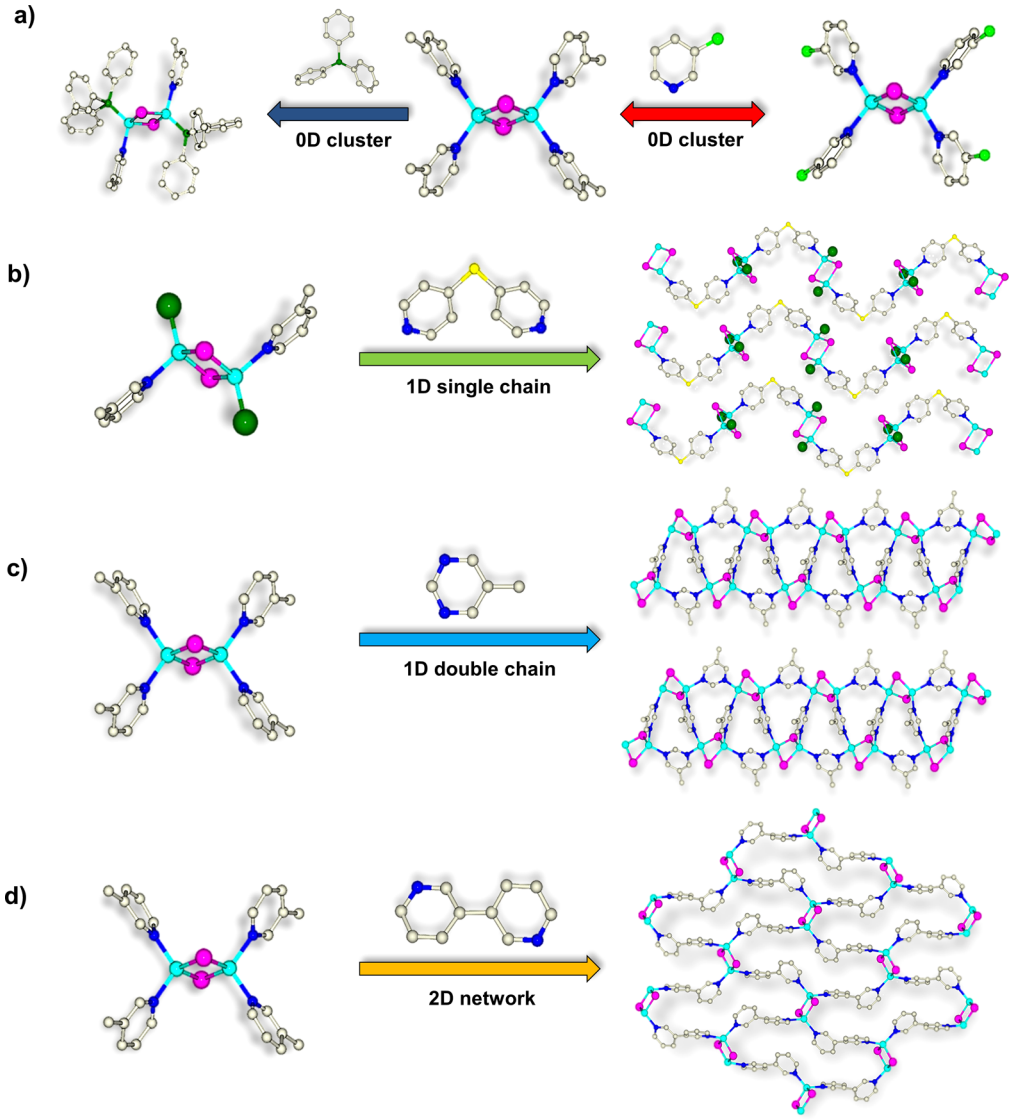

Figure 1. Schematic illustrating the design and construction of CuI(L) hybrid structures with a Cu_2I_2 molecular dimer precursor: (a) 0D cluster, (b)1D single chain, (c) 1D double chain, and (d) 2D layered network. Color scheme of the balls: purple, I; cyan, Cu; dark blue, N; gray, C; light green, Cl; small green, P; large green, tpp molecule.

direct mixing of CuI (in either KI saturated solution or acetonitrile) and ligand often results in mixture phases of several products, making it difficult to isolate the targeted compound. In order to achieve new hybrid structures that combine the desirable properties while avoiding the formation of unwanted phases, we have developed a bottom-up and precursor-based synthetic approach in this study. Our strategy is to construct extended network structures using 0D-$Cu_2I_2(L)_4$ dimers as molecular precursors. We anticipate that these compounds will be strongly emissive, as the dimeric identity is retained in the final product, and highly stable, as a result of high dimensionality. Specifically, the proposed synthesis can be realized by ligand exchange. As shown in Figure 1, ligands with different binding sites, functional groups, shape and size can be selected to control the dimensionality and structure types, while keeping the inorganic motif unchanged. In addition, judiciously selecting ligands with suitable electronic properties (e.g., LUMO energy levels) will allow a systematic tuning of the energy gap of the resulting hybrid compounds as well as their optical emission properties.[39]

0D-$Cu_2I_2(3\text{-pc})_4$ (**1**) was preselected as the precursor, and acetone was selected as the solvent. The latter can effectively dissolve the molecular dimers and allows reactions to proceed in solution and under mild conditions. To confirm that the dimers remain intact in the solution, the solvent was evaporated, and the precipitate was identified by PXRD analysis. This is also fully supported by the absorption spectra taken on both the solid and solution samples of **1** (see Figure S24). Exchange of 3-pc with excess amount of monodentate ligands (L) led to new 0D-$Cu_2I_2(L)_4$ structures (Figure 1a), such as 0D-$Cu_2I_2(3,5\text{-dm-py})_4$ (**2**) and 0D-$Cu_2I_2(3\text{-Cl-py})_4$ (**3**). Phosphines are commonly used to make 0D-$Cu_4I_4(L)$ tetramer-based clusters.[53] In this study we used a common phosphine, triphenylphosphine (tpp), to replace two 3-pc molecules in precursor **1** to form 0D-$Cu_2I_2(tpp)_2(3\text{-pc})_2$ (**4**). Compound **4** was also used as a precursor to synthesize other 0D-$Cu_2I_2(tpp)_2(L)_2$ (e.g., **5**) and 1D-$Cu_2I_2(tpp)_2(L)$ (e.g., **10**) compounds simply by ligand exchange.

The 1D structures were synthesized by two pathways, as illustrated in Figure 1b,c. The 1D single-chain structures can be

DOI: 10.1021/jacs.5b04840
J. Am. Chem. Soc. 2015, 137, 9400−9408

obtained using 0D-$Cu_2I_2(tpp)_2(L)_2$ as the precursor. These include 1D-$Cu_2I_2(tpp)_2$(bpp) (**6**), 1D-$Cu_2I_2(tpp)_2$(4,4′-dps) (**7**), 1D-$Cu_2I_2(tpp)_2$(4,4′-bpy) (**8**), 1D-$Cu_2I_2(tpp)_2$(5-Br-pm) (**9**), and 1D-$Cu_2I_2(tpp)_2$(pz) (**10**). In these structures, the Cu_2I_2 motifs are interconnected by the bidentate nitrogen ligands. The tpp ligand with a stronger Cu−P bond remains unchanged and acts as a terminal ligand in all resulting structures. The 1D double-chain structures were synthesized using 0D-Cu_2I_2(3-pc)$_4$ as the precursor. The four monodentate ligands were exchanged with bidentate ligands, giving rise to 1D-Cu_2I_2(5-me-pm)$_2$ (**11**) and 1D-Cu_2I_2(5-Br-pm)$_2$ (**12**).

The 2D-layered compounds 2D-Cu_2I_2(bpe)$_2$ (**13**), 2D-Cu_2I_2(3,3′-bpy)$_2$ (**14**), 2D-Cu_2I_2(4,4′-dps)$_2$ (**15**), and 2D-Cu_2I_2(4,4′-bpy)$_2$ (**16**) were obtained by exchanging 3-pc in precursor **1** with rod-like bidentate N-ligands (Figure 1d). Usually an excess amount of ligand was used to ensure complete transformation.

As demonstrated above, the precursor approach has two obvious advantages. First, it preserves Cu_2I_2 dimer motifs and their strong luminescence in forming robust network structures. Second, it facilitates the reactions leading to targeted compounds (Figures S5−S7) and effectively eliminates the formation of other types of structures built on different CuI modules which sometimes cannot be avoided using CuI salt as the starting material (see Figure S7a). Phase purity of selected samples was also examined by elemental analysis. Excellent agreement was found between experimental and calculated results (Table S7). In addition, all materials can be synthesized within several hours, and in some cases, in minutes, at room temperature and in solution. The synthesis can easily be scaled up to produce large quantities with only minor modifications. Compared to the previously reported procedures, this method is much more predictable, facile, and energy efficient.

Structure Description. All CuI-based hybrid structures have the general formula $Cu_2I_2(L_1)_m(L_2)_n$. Each Cu in the Cu_2I_2 motif is tetrahedrally coordinated to two iodine atoms and two organic ligands. Depending on the geometry and coordination modes of the ligands, the resulting structures have various dimensionalities, ranging from 0D clusters to 1D single- or double-chains, to 2D networks (see Table 1). The 0D molecular clusters have a general formula of either 0D-$Cu_2I_2(L)_4$ or 0D-$Cu_2I_2(tpp)_2(L)_2$, where both tpp and L are monodentate ligands coordinated to the inorganic motif through either Cu−P or Cu−N bond. Both 1D and 2D structures are built on Cu_2I_2 and bidentate ligands, with a general formula of 1D-$Cu_2I_2(tpp)_2$L and 1D-$Cu_2I_2(L)_2$, respectively. All 2D structures can be formulated as 2D-$Cu_2I_2(L)_2$.

Thermal Stability. High thermal stability is an important criterion for phosphors. Thermal stability of the new hybrid compounds was evaluated by TG analysis (Figure 2a and Figures S15−18). Having decomposition temperatures typically below 100 °C (e.g., 50−60 °C), the molecular (0D) clusters without tpp have the lowest stability (Table 2). Including tpp as the terminal ligand generally enhances structure stability, as a result of the stronger Cu−P bond. Decomposition of structures usually begins with loss of the organic ligand. The remaining residue is identified as copper iodide. As expected, the extended 1D and 2D compounds are significantly more thermally stable than the 0D molecular species due to their extended network structures. Most of them are stable above 150 °C, with some approaching 200 °C (Table 2). The overall trend is 0D < 1D < 2D (Figure 2a). These compounds are also air-stable. Our tests show that samples left in air for several months retain their structures and emission intensity. Their water stability was examined by immersing samples in water for an extended period of time. For example, 200 mg each of 1D-$Cu_2I_2(tpp)_2$(4,4′-dps) (**7**) and 2D-Cu_2I_2(4,4′-dps)$_2$ (**15**) was immersed in water for 24 h and recollected. PXRD analysis confirmed the structural stability with a <5% decrease in luminescence intensity.

Table 1. List of New Cu_2I_2-Based Compounds with Their Unit Cell Parameters and Space Groups

compound	unit cell constants (Å)	space group
0D-Cu_2I_2(3-Cl-py)$_4$ (**3**)	a =7.8020(4)	*P*-1
	b = 8.6628(4)	
	c = 9.4711(5)	
	α = 90.919(2)	
	β = 94.251(3)	
	γ = 102.751(2)	
0D-$Cu_2I_2(tpp)_2$(3-pc)$_2$ (**4**)	a = 25.9199(15)	*C*2/*c*
	b =14.9505(9)	
	c = 11.5468(7)	
	β = 97.115(2)	
0D-$Cu_2I_2(tpp)_2$(4,6-dm-pm)$_2$ (**5**)	a = 9.3886(3)	*P*-1
	b = 11.5199(4)	
	c = 11.5849(4)	
	α = 79.129(2)	
	β = 69.089(2)	
	γ = 72.439(2)	
1D-$Cu_2I_2(tpp)_2$(bpp) (**6**)	a = 13.2151(5)	$P2_1/c$
	b =13.5525(5)	
	c = 25.3512(9)	
	β = 94.613(2)	
1D-$Cu_2I_2(tpp)_2$(4,4′-dps) (**7**)	a = 26.0237(10)	*C*2/*c*
	b =9.3012(4)	
	c = 20.2799(8)	
	β = 117.533(2)	
1D-$Cu_2I_2(tpp)_2$(5-Br-pm) (**9**)	a = 17.2033(7)	*C*2/*c*
	b =17.7719(7)	
	c = 14.9470(6)	
	β = 122.467(2)	
1D-Cu_2I_2(5-me-pm)$_2$ (**11**)	a = 8.4063(4)	*Cmca*
	b =21.6785(10)	
	c = 16.5331(7)	
1D-Cu_2I_2(5-Br-pm)$_2$ (**12**)	a = 8.437(2)	*Cmca*
	b = 21.875(6)	
	c = 16.757(4)	
2D-Cu_2I_2(3,3′-bpy)$_2$ (**14**)	a = 9.4898(13)	$P2_1/n$
	b = 9.7370(18)	
	c = 12.2051(18)	
	β = 111.784(2)	

Band Gaps and Optical Tunability. Experimental optical absorption spectra of selected 0D, 1D, and 2D structures are plotted in Figure 2b. The band gap values estimated from the absorption data are listed in Table 2. DFT calculations were conducted on several selected structures, and the results are summarized in Figure 3 and Supporting Information. From both sets of data the same trend is derived (Figure 3, Figures S19−S23, and Table S3). As in the case of staircase-like chain structures of 1D-CuI(L),[39] the valence band maximum (VBM) consists primarily of the atomic states of inorganic components (Cu 3d and I 5p), while the conduction band minimum (CBM) is composed mainly of the atomic states that make up the

DOI: 10.1021/jacs.5b04840
J. Am. Chem. Soc. 2015, 137, 9400−9408

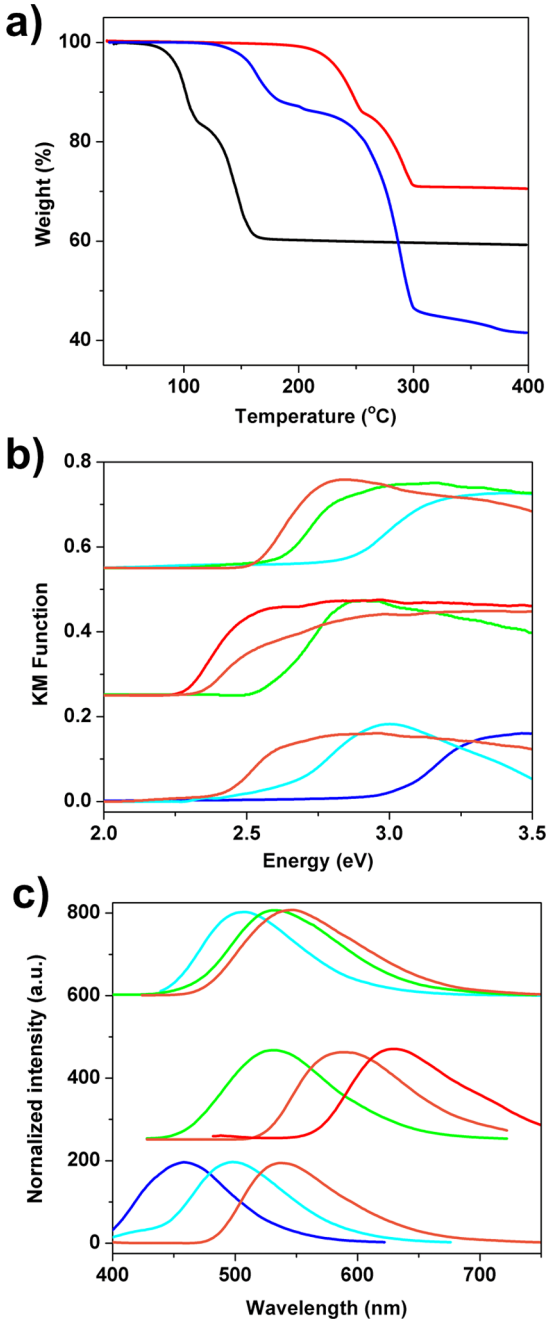

Figure 2. (a) TG profiles of selected 0D, 1D, and 2D structures: **1** (black), **8** (blue), and **14** (red). (b) Optical absorption spectra of selected 0D (bottom), 1D (middle), and 2D (upper) structures. Bottom: **4** (blue), **1** (cyan), **3** (orange). Middle: **7** (green), **11** (orange), **12** (red). Top: **13** (cyan), **14** (green), **15** (orange). These colors coincide with their emission colors. (c) PL spectra (λ_{ex} = 360 nm) of compounds given in (b).

lowest unoccupied molecular orbitals (LUMOs) of organic ligands (C 2p and N 2p). As the photo excitation process in these hybrid compounds involves electron transfer from the VBM (mostly inorganic) to CBM (mostly organic) states, their emission energies correlates to the LUMOs of the ligands. Therefore, incorporating ligands with suitable LUMO energies allows us to systematically tune the energy gap of resulting hybrid structures and, consequently, their photoluminescence (PL). Taking compounds **13**–**16** as an example, all belong to the 2D-$Cu_2I_2(L)_2$ structure type. Their experimental band gaps are estimated to be 2.8, 2.6, 2.5, and 2.0 eV, respectively, correlating fully with the decreasing LUMO energy of the corresponding ligands, −1.244, −1.654, −1.790, and −2.044 eV, calculated using the 6-311++G(3df,3pd) basis set (Tables S4 and S6). Similarly, calculations on another selected group of 0D structures, **2**–**4**, gave the same matching trend for their energy gaps, emission energies, and the LUMOs of the ligands (Tables S5 and S6 and Figures S19–S21). For structures containing tpp and N-ligand, both molecules contribute to the CBM region (Figure 3a, Figure S21), and as a result, the energy levels of CBM are affected by both ligands.

Photoluminescence, Quantum Efficiency, and Color Quality. Experimental PL data collected at room temperature show that the emission of these hybrid compounds is typically single band, with a full width at half-maximum (fwhm) of ∼around 100 nm (Figure 2c). The emission color ranges from blue to red, spanning the entire visible region (Figures 2c and 4b and Table 2). The emission energies are in trend with their band gap values with a stoke shift in the range from 70 to 100 nm. Note that the high IQYs observed in molecular Cu_2I_2 dimers are retained in most of the dimer-based extended 1D and 2D structures with similar band/energy gaps, with a majority of them exceeding 70% and as high as 92% (Table 2). For a given structure type, compounds with higher band gaps have higher IQYs than those with lower band gaps, in accordance with the energy gap law.[54] For example, among the 1D-$Cu_2I_2(tpp)_2(L)$ structures, members with higher band gaps such as **6** and **7** (band gap: 2.6–2.8 eV) have IQYs of 91.7% and 80.0%, respectively, while for the members with lower band gaps such as **9** and **10** (band gap: 2.1–2.3 eV), the values are significantly lower at only 26.1 and 30.8%. Based on $\Phi = k_r\tau$ (where Φ is quantum yield, τ is lifetime, k_r is radiative rate constant),[55] quantum yield is directly proportional to the lifetime. Luminescence decay measurements were carried out on selected compounds **6** and **15** and also compared with reported values of **8** and **10**.[44] Their τ values are 13.1, 6.5, 4.0, and 1.7 μs for **6**, **15**, **8**, **10**, respectively, in trend with their deceasing band gap values of 2.8, 2.5, 2.4, and 2.1 eV as well as their quantum yield values of **6** > **8**, **15** ≫ **10** (Figures S25 and S26 and Table S5).

As blue-excitable yellow phosphors are an essential component for the current WLED technologies, we have paid special focus to developing these compounds as possible alternatives for the commercial RE-based yellow phosphor YAG:Ce^{3+} (Ce-doped yttrium aluminum garnet). Several members of the family represent promising candidates, including compounds **8** and **15**, with IQYs as high as ∼70% when excited by blue light (455 nm). As a comparison, the emission spectra of **15** and YAG:Ce^{3+} are plotted in Figure 4a. Both have a broad band emission in the yellow region with a slight red shift in emission energy for **15** ("yellower"). The CIE coordinates were calculated to be (0.40, 0.54) and (0.41, 0.56) for **15** and YAG:Ce^{3+}, respectively.

A series of thermal, moisture, and photo stability experiments were further performed to test the suitability of **15** as a candidate for WLED (Figures S27 and S28). The PXRD analysis on a sample of **15** exposed to air for 6 months or dispersed in water for 1 day revealed no structure change and emission intensity dropped <5%. Similarly, a sample under blue light (455 nm) for a week showed no obvious changes either in its PXRD pattern or emission intensity. Furthermore, heating the sample at 80 °C for 1 week did not lead to apparent

DOI: 10.1021/jacs.5b04840
J. Am. Chem. Soc. 2015, 137, 9400–9408

Table 2. Estimated Band Gaps, Emission Energies and IQY, Emission Color of Cu_2I_2-Based Compounds, and LUMO Energies of Organic Ligands Calculated at the Level of B3LYP/6-311++G(3df,3pd)

compounds	band gap (eV)	λ_{em} (nm)	emission color	CIE	IQY (%)	decomposition temp. (°C)
0D-Cu_2I_2(3-pc)$_4$ (**1**)	2.6	496	blue-green	0.21, 0.40	95.2 ± 1.4	60
0D-Cu_2I_2(3,5-dm-py)$_4$ (**2**)	2.8	479	blue	0.17, 0.24	81.5 ± 1.1	60
0D-Cu_2I_2(3-Cl-py)$_4$ (**3**)	2.5	530	green	0.38, 0.58	85.6 ± 1.2	50
0D-Cu_2I_2(tpp)$_2$(3-pc)$_2$ (**4**)	3.0	455	blue	0.14, 0.15	90.3 ± 0.4	135
0D-Cu_2I_2(tpp)$_2$(4,6-dm-pm)$_2$ (**5**)	2.9	465	blue	0.15, 0.17	72.3 ± 0.2	120
1D-Cu_2I_2(tpp)$_2$(bpp) (**6**)	2.8	458	blue	0.15, 0.15	91.7 ± 0.5	180
1D-Cu_2I_2(tpp)$_2$(4,4′-dps) (**7**)	2.6	532	green-yellow	0.33, 0.54	80.0 ± 1.2	150
1D-Cu_2I_2(tpp)$_2$(4,4′-bpy) (**8**)	2.4	540	yellow	0.38, 0.58	76.2 ± 0.9	160
1D-Cu_2I_2(tpp)$_2$(pz) (**10**)	2.1	631	red	0.55, 0.30	26.1 ± 0.3	120
1D-Cu_2I_2(5-me-pm)$_2$ (**11**)	2.3	570	orange	0.43, 0.53	30.8 ± 0.8	130
2D-Cu_2I_2(bpe)$_2$ (**13**)	2.8	494	blue-green	0.20, 0.37	82.3 ± 0.4	170
2D-Cu_2I_2(3,3′-bpy)$_2$ (**14**)	2.6	515	green	0.26, 0.50	77.3 ± 0.6	210
2D-Cu_2I_2(4,4′-dps)$_2$ (**15**)	2.5	547	yellow	0.40, 0.54	70.8 ± 0.3	160
Two-component white phosphor (**17**)	–	458, 540	white	0.31, 0.36	62.6 ± 0.2	160

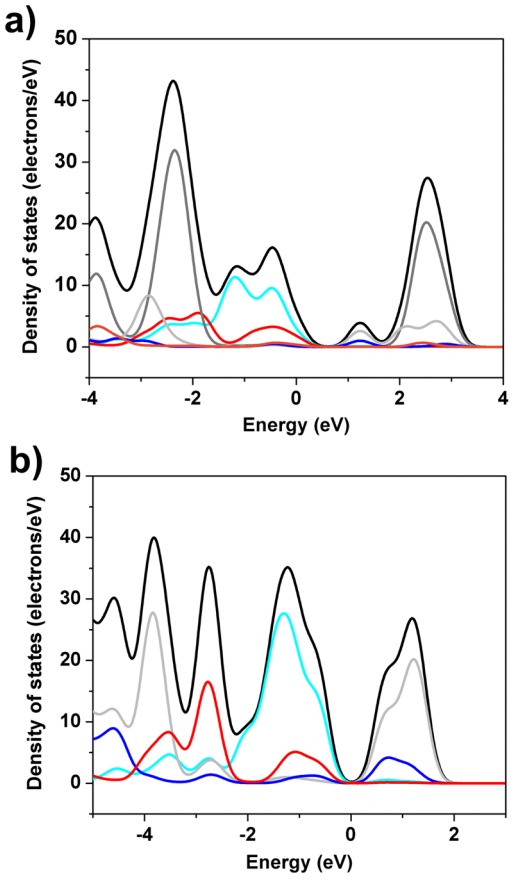

Figure 3. Calculated DOS for (a) **8** and (b) **15**: total DOS (black); Cu 3d orbitals (light blue); I 5p orbitals (red); N 2p orbitals (blue); P 3p orbitals (orange); C from N-ligand 2p orbitals (light gray); and C from tpp 2p orbitals (gray). The maximum of the valence band is set at 0 eV.

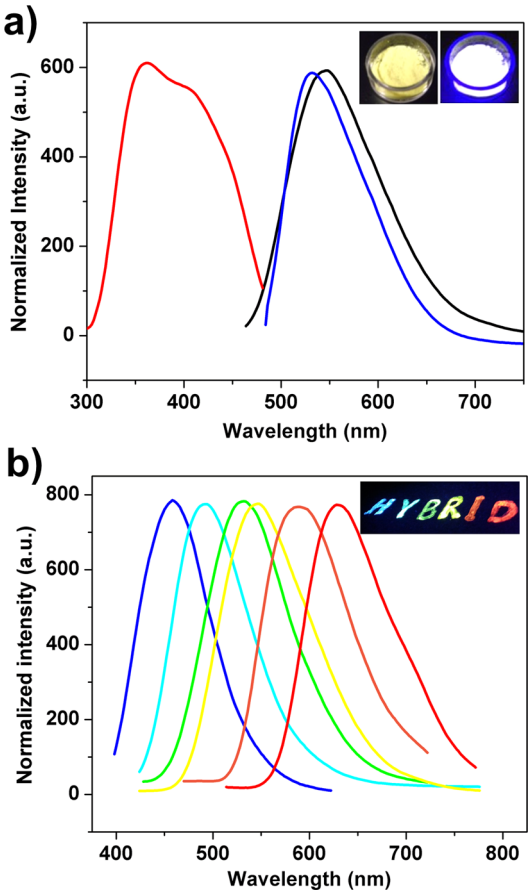

Figure 4. (a) Excitation (red, λ_{em} = 543 nm) and emission (black, λ_{ex} = 455 nm) spectra of **15** compared with emission spectrum of YAG:Ce^{3+} (blue, λ_{ex} = 455 nm). Inset: powder sample of **15** under natural light (left) and blue light (right, 455 nm). (b) PL spectra of selected compounds, spanning the whole visible light region. From left to right: **4**, **13**, **7**, **15**, **9**, and **10**. Inset: coating of these samples on black substrate, exposed to UV light. λ_{ex} 360 nm.

structure change, and the decrease in the emission intensity was negligible.

In addition to yellow phosphors, RE-free phosphors of other colors are also highly desirable for the general lighting industry, such as blue, green and red phosphors commonly used in CFLs.[56] Red phosphors are also commonly used in combination with YAG:Ce^{3+} in WLEDs to achieve warmer white light.[57] The Cu_2I_2-based hybrid phosphors have the unique advantage of optical tunability achieved by using ligands with targeted LUMO energies. This gives rise to a full color spectrum covering the entire visible region (Figure 4b and Table 2).

Two-component white phosphors were made by mechanically blending a blue-emitting phosphor (e.g., **6**) with a yellow-

DOI: 10.1021/jacs.5b04840
J. Am. Chem. Soc. 2015, 137, 9400–9408

emitting phosphor (e.g., **8**). The two compounds have very similar structures and thus are highly compatible. Depicted in Figure 5a are the emission spectra of three mixtures with

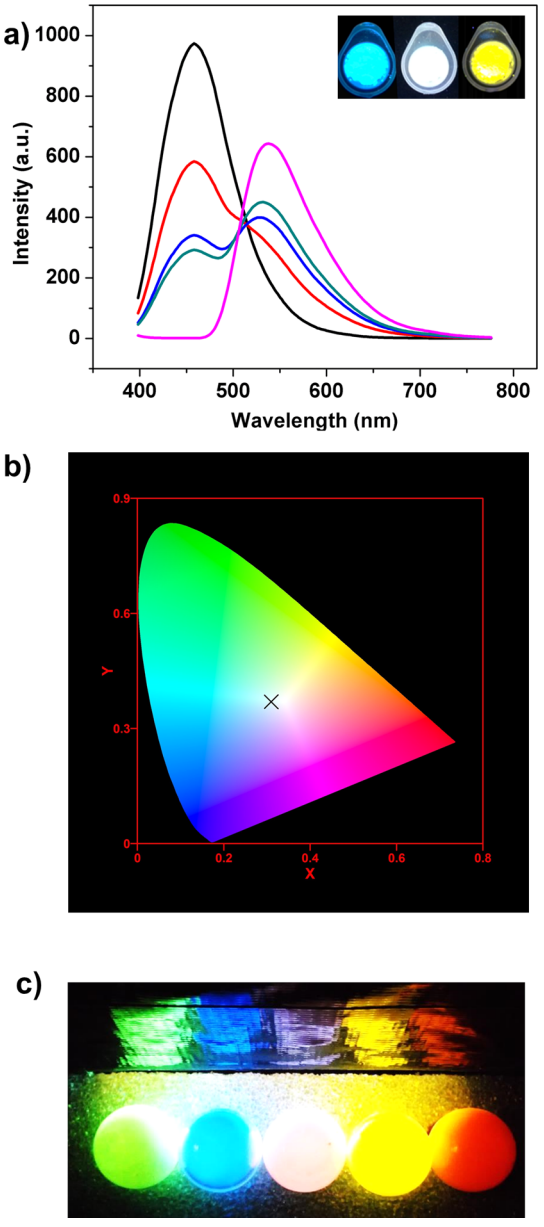

Figure 5. (a) Luminescence spectra of the two-component phosphors with the following weight percentage of **8**: 0 wt % (black), 5 wt % (red), 15 wt % (blue), 25 wt % (green), 100 wt % (pink). λ_{ex} = 360 nm. Inset: powder samples under UV irradiation. From left to right: 0, 25, and 100 wt %. (b) CIE coordinates of **17** (25 wt % of **8**). (c) LED bulbs displayed at working condition.

selected compositions as well as those of pure **6** and **8**. The overall emission profile and white color depend on the relative amount of the two phosphors. An optimum composition was found to be 25 wt % of **8** or compound **17**. Its IQY, CIE, color rendering index, and correlated color temperature are 62.6%, (0.31, 0.36), 73.8, and 4512 K, respectively, representing a well-balanced white color (Figure 5b and Table S6).

To further evaluate the performance of hybrid phosphors, LED bulbs were fabricated using the remote phosphor coating design, where the phosphors were physically separated from the LED chip. A water-soluble binder (PolyOx N-750) was used for the phosphor coating. The phosphors were coated on the inner surface of 25 mm diameter glass globes. Violet (405 nm) or blue (455 nm) LEDs were used as the excitation source inside the bulb. A schematic of this system is illustrated in Figure S29. Figure 5c is the image of the bulbs taken at the working condition.

CONCLUSION

In summary, we have developed a bottom-up precursor approach to aid in the rational design pathway for the creation of copper iodide based RE-free hybrid phosphors. This approach allows integration of three important and targeted properties in the new hybrid series formed: (a) exceptionally strong luminescence and high quantum yield as a result of preservation of highly emissive Cu_2I_2 module; (b) systematic optical tunability due to the incorporation of a vast number of organic ligands; and (c) significantly enhanced framework stability by means of formation of extended networks. The new phosphors have a number of apparent advantages in comparison with commercial phosphors, as they can be synthesized by low-cost, solution-based, easily scalable, and fully controllable routes at room temperature. They are totally free of rare-earth elements, and their emission energy and color can be systematically and finely tuned. Their high quantum efficiency (up to 95%) is comparable to that of the commercial phosphors. This work demonstrates the potential to develop highly efficient, rare-earth-free phosphor alternatives made of inexpensive earth abundant elements that are promising for use in general lighting technologies.

ASSOCIATED CONTENT

Supporting Information

Crystallographic data, PXRD patterns, TGA data, PL spectra, and DFT calculation results. The Supporting Information is available free of charge on the ACS Publications website at DOI: 10.1021/jacs.5b04840.

AUTHOR INFORMATION

Corresponding Author

*jingli@rutgers.edu

Author Contributions

‖These authors contributed equally.

Notes

The authors declare no competing financial interest.

ACKNOWLEDGMENTS

Financial support from the National Science Foundation (grant no. DMR-1206700 and DMR-1507210) is gratefully acknowledged. The Advanced Light Source (ALS) is supported by the Director, Office of Science, Office of Basic Energy Science, of the U.S. Department of Energy, under contract DE-AC02-05CH11231. W.L. would like to thank Dechao Yu for helpful discussions. G.Z.W. acknowledges fellowship support from the Rutgers University Aresty Research Center and Rutgers Energy Institute (REI).

REFERENCES

(1) Pimputkar, S.; Speck, J. S.; DenBaars, S. P.; Nakamura, S. *Nat. Photonics* **2009**, *3*, 180.

(2) Khan, N.; Abas, N. *Renewable Sustainable Energy Rev.* **2011**, *15*, 296.

DOI: 10.1021/jacs.5b04840
J. Am. Chem. Soc. 2015, 137, 9400−9408

(3) Aman, M. M.; Jasmon, G. B.; Mokhlis, H.; Bakar, A. H. A. *Energy Policy* **2013**, *52*, 482.
(4) Reineke, S.; Lindner, F.; Schwartz, G.; Seidler, N.; Walzer, K.; Luessem, B.; Leo, K. *Nature* **2009**, *459*, 234.
(5) Lim, S.-R.; Kang, D.; Ogunseitan, O. A.; Schoenung, J. M. *Environ. Sci. Technol.* **2013**, *47*, 1040.
(6) Yadav, P. J.; Joshi, C. P.; Moharil, S. V. *J. Lumin.* **2013**, *136*, 1.
(7) Ye, S.; Xiao, F.; Pan, Y. X.; Ma, Y. Y.; Zhang, Q. Y. *Mater. Sci. Eng., R* **2010**, *71*, 1.
(8) Krames, M. R.; Shchekin, O. B.; Mueller-Mach, R.; Mueller, G. O.; Ling, Z.; Harbers, G.; Craford, M. G. *J. Disp. Technol.* **2007**, *3*, 160.
(9) Hoppe, H. A. *Angew. Chem., Int. Ed.* **2009**, *48*, 3572.
(10) Song, Y. H.; Jia, G.; Yang, M.; Huang, Y. J.; You, H. P.; Zhang, H. J. *Appl. Phys. Lett.* **2009**, *94*, 091902.
(11) Setlur, A. A. *Electrochem. Soc. Interface* **2009**, *16*, 32.
(12) Bradsher, K. The New York Times, 2010.
(13) Shi, H. L.; Zhu, C.; Huang, J. Q.; Chen, J.; Chen, D. C.; Wang, W. C.; Wang, F. Y.; Cao, Y. G.; Yuan, X. Y. *Opt. Mater. Express* **2014**, *4*, 649.
(14) Haranath, D.; Chander, H.; Sharma, P.; Singh, S. *Appl. Phys. Lett.* **2006**, *49*, 173118.
(15) Rinehart, J. D.; Schimpf, A. M.; Weaver, A. L.; Cohn, A. W.; Gamelin, D. R. *J. Am. Chem. Soc.* **2013**, *135*, 18782.
(16) Dai, Q. Q.; Duty, C. E.; Hu, M. Z. *Small* **2010**, *6*, 1577.
(17) Bowers, M. J.; McBride, J. R.; Rosenthal, S. J. *J. Am. Chem. Soc.* **2005**, *127*, 15378.
(18) Kim, S.; Kim, T.; Kang, M.; Kwak, S. K.; Yoo, T. W.; Park, L. S.; Yang, I.; Hwang, S.; Lee, J. E.; Kim, S. K.; Kim, S. W. *J. Am. Chem. Soc.* **2012**, *134*, 3804.
(19) Tanaka, M.; Sawai, S.; Sengoku, M.; Kato, M.; Masumoto, Y. *J. Appl. Phys.* **2000**, *87*, 8535.
(20) Ghosh, Y.; Mangum, B. D.; Casson, J. L.; Williams, D. J.; Htoon, H.; Hollingsworth, J. A. *J. Am. Chem. Soc.* **2012**, *134*, 9634.
(21) Liang, R.; Yan, D.; Tian, R.; Yu, X.; Shi, W.; Li, C.; Wei, M.; Evans, D. G.; Duan, X. *Chem. Mater.* **2014**, *26*, 2595.
(22) Xuan, T.-T.; Liu, J.-Q.; Xie, R.-J.; Li, H.-L.; Sun, Z. *Chem. Mater.* **2015**, *27*, 1187.
(23) Kagan, C. R.; Mitzi, D. B.; Dimitrakopoulos, C. D. *Science* **1999**, *286*, 945.
(24) Fang, X.; Roushan, M.; Zhang, R.; Peng, J.; Zeng, H.; Li, J. *Chem. Mater.* **2012**, *24*, 1710.
(25) Zhang, R.; Emge, T. J.; Zheng, C.; Li, J. *J. Mater. Chem. A* **2013**, *1*, 199.
(26) Li, J.; Bi, W.; Ki, W.; Huang, X.; Reddy, S. *J. Am. Chem. Soc.* **2007**, *129*, 14140.
(27) Roushan, M.; Zhang, X.; Li, J. *Angew. Chem., Int. Ed.* **2012**, *51*, 436.
(28) Ki, W.; Li, J.; Eda, G.; Chhowalla, M. *J. Mater. Chem.* **2010**, *20*, 10676.
(29) Huang, X. Y.; Li, J. *J. Am. Chem. Soc.* **2007**, *129*, 3157.
(30) Huang, X. Y.; Li, J.; Zhang, Y.; Mascarenhas, A. *J. Am. Chem. Soc.* **2003**, *125*, 7049.
(31) Ki, W.; Li, J. *J. Am. Chem. Soc.* **2008**, *130*, 8114.
(32) Zhang, X.; Hejazi, M.; Thiagarajan, S. J.; Woerner, W. R.; Banerjee, D.; Emge, T. J.; Xu, W.; Teat, S. J.; Gong, Q.; Safari, A.; Yang, R.; Parise, J. B.; Li, J. *J. Am. Chem. Soc.* **2013**, *135*, 17401.
(33) Yao, H.-B.; Gao, M.-R.; Yu, S.-H. *Nanoscale* **2010**, *2*, 323.
(34) Gao, M.-R.; Yao, W.-T.; Yao, H.-B.; Yu, S.-H. *J. Am. Chem. Soc.* **2009**, *131*, 7486.
(35) Zheng, N.; Bu, X.; Lu, H.; Chen, L.; Feng, P. *J. Am. Chem. Soc.* **2005**, *127*, 14990.
(36) Turekian, K. K. *McGraw-Hill Encyclopedia of Science and Technology*; McGraw-Hill: New York, 1970; Vol. *4*.
(37) Ford, P. C.; Cariati, E.; Bourassa, J. *Chem. Rev.* **1999**, *99*, 3625.
(38) Liu, Z.; Qayyum, M. F.; Wu, C.; Whited, M. T.; Djurovich, P. I.; Hodgson, K. O.; Hedman, B.; Solomon, E. I.; Thompson, M. E. *J. Am. Chem. Soc.* **2011**, *133*, 3700.
(39) Zhang, X.; Liu, W.; Wei, G. Z.; Banerjee, D.; Hu, Z.; Li, J. *J. Am. Chem. Soc.* **2014**, *136*, 14230.
(40) Tsuge, K.; Chishina, Y.; Hashiguchi, H.; Sasaki, Y.; Kato, M.; Ishizaka, S.; Kitamura, N. *Coord. Chem. Rev.*
(41) Rath, N. P.; Maxwell, J. L.; Holt, E. M. *J. Chem. Soc., Dalton Trans.* **1986**, 2449.
(42) Healy, P. C.; Pakawatchai, C.; White, A. H. *J. Chem. Soc., Dalton Trans.* **1983**, 1917.
(43) Li, R.-Z.; Li, D.; Huang, X.-C.; Qi, Z.-Y.; Chen, X.-M. *Inorg. Chem. Commun.* **2003**, *6*, 1017.
(44) Araki, H.; Tsuge, K.; Sasaki, Y.; Ishizaka, S.; Kitamura, N. *Inorg. Chem.* **2005**, *44*, 9667.
(45) Yang, Z.; Chen, Y.; Chun-Yan, N.; Ren, Z.-G.; Wang, H.-F.; Li, H.-X.; Lang, J.-P. *Inorg. Chem. Commun.* **2011**, *14*, 1537.
(46) Muthu, S.; Ni, Z.; Vittal, J. J. *Inorg. Chim. Acta* **2005**, *358*, 595.
(47) Batten, S. R.; Jeffery, J. C.; Ward, M. D. *Inorg. Chim. Acta* **1999**, *292*, 231.
(48) Bril, A.; de Jager-Veenis, A. W. *J. Electrochem. Soc.* **1976**, *123*, 396.
(49) Bai, X.; Caputo, G.; Hao, Z.; Freitas, V. T.; Zhang, J.; Longo, R. L.; Malta, O. L.; Ferreira, R. A. S.; Pinna, N. *Nat. Commun.* **2014**, *5*, 5702.
(50) Lee, C.; Yang, W.; Parr, R. G. *Phys. Rev. B: Condens. Matter Mater. Phys.* **1988**, *37*, 785.
(51) Frisch, M. J.; Trucks, G. W.; Schlegel, H. B.; Scuseria, G. E.; Robb, M. A.; Cheeseman, J. R.; Scalmani, G.; Barone, V.; Mennucci, B.; Petersson, G. A.; Nakatsuji, H.; Caricato, M.; Li, X.; Hratchian, H. P.; Izmaylov, A. F.; Bloino, J.; Zheng, G.; Sonnenberg, J. L.; Hada, M.; Ehara, M.; Toyota, K.; Fukuda, R.; Hasegawa, J.; Ishida, M.; Nakajima, T.; Honda, Y.; Kitao, O.; Nakai, H.; Vreven, T.; Montgomery, J. A., Jr.; Peralta, J. E.; Ogliaro, F.; Bearpark, M.; Heyd, J. J.; Brothers, E.; Kudin, K. N.; Staroverov, V. N.; Kobayashi, R.; Normand, J.; Raghavachari, K.; Rendell, A.; Burant, J. C.; Iyengar, S. S.; Tomasi, J.; Cossi, M.; Rega, N.; Millam, J. M.; Klene, M.; Knox, J. E.; Cross, J. B.; Bakken, V.; Adamo, C.; Jaramillo, J.; Gomperts, R.; Stratmann, R. E.; Yazyev, O.; Austin, A. J.; Cammi, R.; Pomelli, C.; Ochterski, J. W.; Martin, R. L.; Morokuma, K.; Zakrzewski, V. G.; Voth, G. A.; Salvador, P.; Dannenberg, J. J.; Dapprich, S.; Daniels, A. D.; Farkas, Ö.; Foresman, J. B.; Ortiz, J. V.; Cioslowski, J.; Fox, D. J. *Gaussian 09*, Revision C.01, Gaussian, Inc.: Wallingford, CT, 2010.
(52) Becke, A. D. *J. Chem. Phys.* **1993**, *98*, 5648.
(53) Perruchas, S.; Goff, X. F. L.; Maron, S.; Maurin, I.; Guillen, F.; Garcia, A.; Gacoin, T.; Boilot, J.-P. *J. Am. Chem. Soc.* **2010**, *132*, 10967.
(54) Englman, R.; Jortner, J. *Mol. Phys.* **1970**, *18*, 145.
(55) Lakowicz, J. R. *Anal. Biochem.* **2001**, *298*, 1.
(56) Sommerer, T. J.; Srivastava, A. M. *Electrochem. Soc. Interface* **1998**, *7*, 28.
(57) Pust, P.; Weiler, V.; Hecht, C.; Tücks, A.; Wochnik, A. S.; Henß, A.-K.; Wiechert, D.; Scheu, C.; Schmidt, P. J.; Schnick, W. *Nat. Mater.* **2014**, *13*, 891.

DOI: 10.1021/jacs.5b04840
J. Am. Chem. Soc. 2015, 137, 9400−9408